

Sensor and Simulation Notes

Note 419

E Field Measurements for a 1meter Diameter Half IRA

Leland H. Bowen
Everett G. Farr
Farr Research, Inc.

April 1998

Abstract

A Half Impulse Radiating Antenna (HIRA) was constructed from one half of an aluminum 1 m diameter parabolic dish with a focal length of 0.383 m. The HIRA had two feed arms with a combined impedance in air of 100Ω .

The step function response of the HIRA was measured in the time domain using a TEM horn sensor. The radiated field in V/m was computed from the raw voltage by deconvolution with the impulse response of the TEM sensor.

The radiated field measurements at 3, 10, and 20 meters are in good agreement with numerical predictions. The HIRA was further characterized by recording the TDR of the antenna, by tabulating the half power and half voltage spot size at 20 m, and by computing the impulse response of the antenna in both the time and frequency domains. The effective height of the HIRA was approximately 0.13 m.

1. Introduction

An Impulse Radiating Antenna (IRA) was designed by Farr Research, Inc. and fabricated by Science Design Inc. (SDI). The antenna was constructed from one half of an aluminum 1 m diameter (D) parabolic dish with a focal length (F) of 0.383 m. This makes the $F/D = 0.383$. The half parabola was mounted on an aluminum ground plane through the axis of the parabola. The Half IRA (HIRA) has two feed arms at 45° to the ground plane as viewed from the front with a combined impedance in air of 100Ω . This makes $f_g^{HIRA} = 100/377 = 0.265$. Each feed arm has a $200\ \Omega$ termination resistor located near the attachment point to the parabolic dish. The termination resistor is made up of five $1000\ \Omega$ resistors in parallel. Each resistor is 1/8 watt with a tolerance of 5%. The HIRA which is a scale model of a 2 m diameter version presently under construction is shown in Figures 1.1 and 1.2.

The radiated field measurements were performed out of doors in an area free of obstructions. The HIRA and the TEM horn sensor were mounted on aluminum tripods with a height above the ground of approximately 1.7m. The source was a Picosecond Pulse Labs Model 4015C which has a 4 volt output with an 18 ps rise time. The measured rise time due to cable and instrument characteristics was 25 – 28 ps as shown in Figure 4.5 of Sensor and Simulation Note (SSN) #413 [1]. The measurements were made using a Tektronix 11801B digitizing oscilloscope with a SD24 TDR head.

The impulse response of the TEM sensor is shown in SSN #413 Figure 4.8 [1]. The impulse response of the TEM sensor was reevaluated for this test with two TEM sensors spaced 10 m apart ($r = 10$). The impulse response and its integral are shown in Figures 1.3 and 1.4. The effective height of the TEM sensor from the integral is approximately 17 mm.



Figure 1.1. Model HIRA

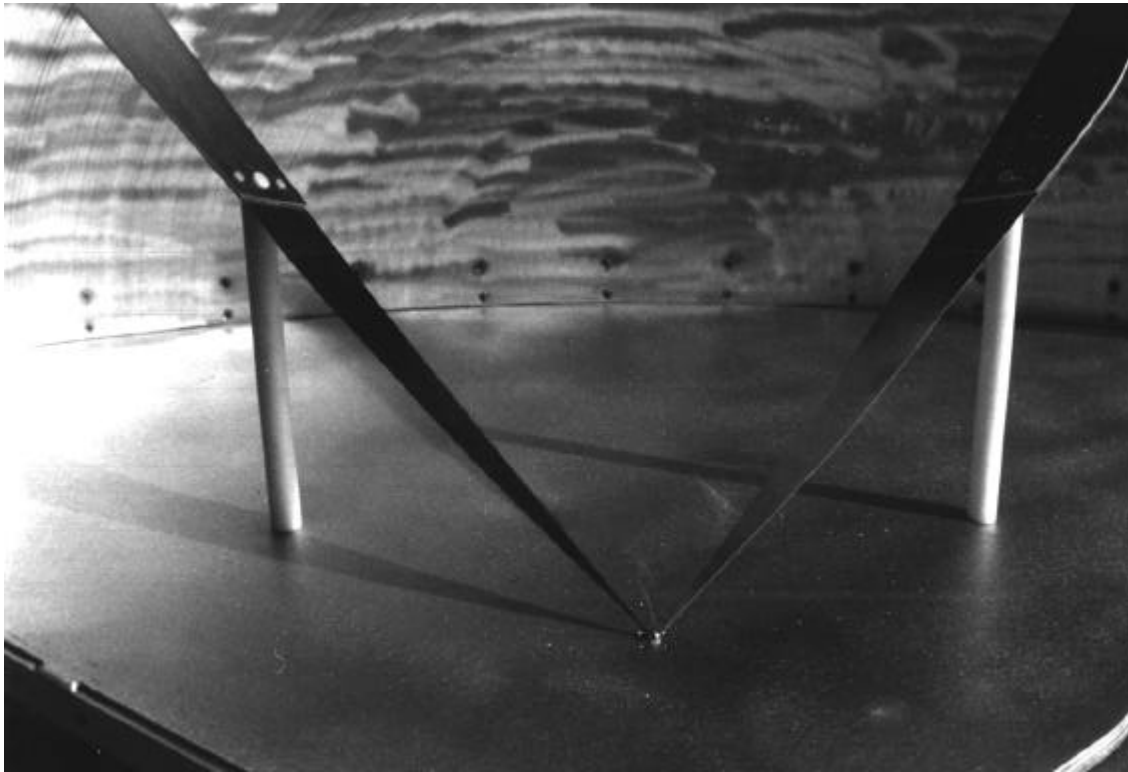


Figure 1.2. Model HIRA

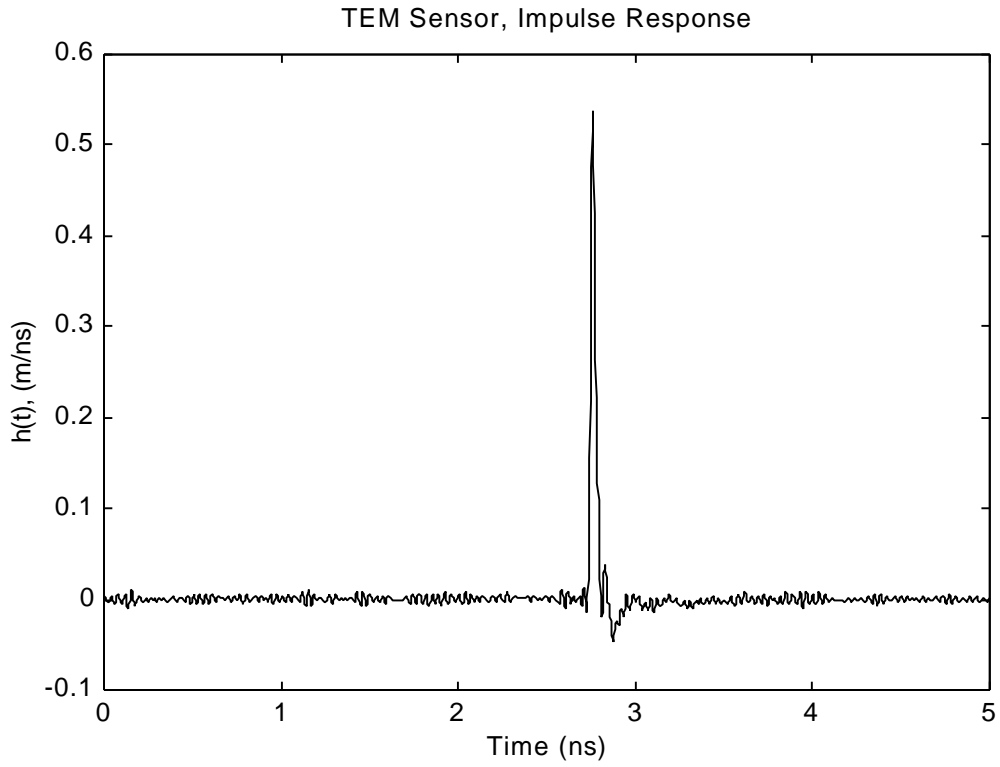


Figure 1.3. $h_{\text{TEM}}(t)$.

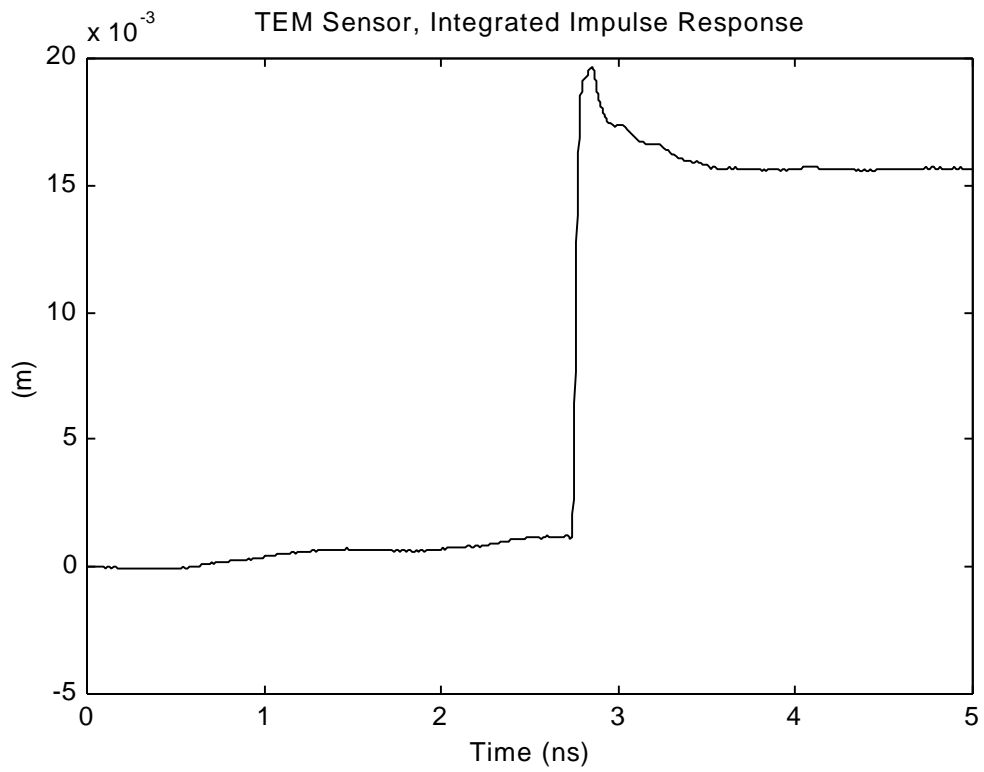


Figure 1.4. $\int h_{\text{TEM}}(t) dt$, Effective Height $\gg 17\text{mm}$.

2. Data

The TDR shown in Figure 2.1 gives the impedance of the HIRA versus time. The first jump in the waveform (to 50 Ω) occurs at the output of the TDR head where it is connected to a 50 Ω cable. The next jump occurs at the feed point of the HIRA. The two feed arms have a combined impedance of 100 Ω . The drop in the impedance occurs at the load resistor location.

The HIRA impulse response ($h_{TEM}(t)$) and integral extracted from data on boresight at 20 m are shown in Figures 2.2 and 2.3. The impulse response of the HIRA was backed out of the equation

$$V_{REC}(t) = \frac{t}{2\pi r c f_{g,HIRA}} \circ h_{TEM}(t) \circ h_{HIRA}(t) \circ dV_{SRC}/dt \quad (1)$$

where the voltage transfer coefficient $t = 2*100/(50+100) = 1.33$. The *FWHM* of the impulse response is 30 ps which is better than the goal of 33 ps. The effective height of the HIRA should be approximately 80% of the term $a/2\sqrt{2}$ where $a = 0.5$ m (the radius of the antenna). This gives 0.14 m. The effective height of the HIRA which is the peak of the integral as shown in Figure 2.3 is 0.13 m. The response in the frequency domain is shown in Figure 2.4.

The radiated field was measured at $r = 3, 10,$ and 20 m. At each distance the field was scanned in both the H and E planes at $0^\circ, 2^\circ, 5^\circ, 7.5^\circ,$ and 15° . The E plane scan for the 3 m case was performed at $2^\circ, 3.8^\circ, 5.7^\circ, 7.6^\circ,$ and 9.5° . These angles correspond to raising the sensor above the level of the ground plane in steps of 10 cm. For convenience, the TEM horn was used as the transmitter and the HIRA used as the receiver. The plots shown here are grouped according to distance. At each distance, the raw data on boresight (0°) is shown first followed by the corrected data. The data correction was performed by deconvolving the raw data with $h_{TEM}(t)$ using a modified Butterworth filter to reduce the noise and limiting the denominator term to prevent division by very small numbers. The corrected data are compared with the predictions made by Dr. David Giri of Pro-Tech [2]. Dr. Giri's calculations are based on a method of calculating pulse radiation from an antenna with a reflector by Mikheev [3]. The model used by Dr. Giri is valid only for the 0° case where the sensor is on the same plane as the truncated ground-plane of the HIRA. This is the case for the comparisons shown in Figures 2.6, 2.10, and 2.19. Dr. Carl Baum shows in [4] that, due to symmetry conditions for the 0° case, the model gives exact results out to the ground-plane clear time.

The 10 m case includes two sets of additional data not shown at 3 and 20 m. Normally the HIRA was turned to the right for the H plane scan and aimed downward for the E plane scan. For the 10 m case, scans to the left and skyward (sensor below the ground plane) are included for comparison. Also, for this case, a comparison of three ground plane configurations is included. Add-on sections were made for the HIRA to provide a rounded or elliptical front edge and a rectangular front edge for the ground plane. Without the add-on sections the ground plane is triangular in shape. This is the normal configuration for the measurements and corrected data presented here. The raw data for the three ground plane configurations are shown in Figures 2.14 – 2.16. Since the measured voltages were almost identical for the three ground plane configurations, no further data were collected or processing performed using the add-on sections.

For the 20 m case the ground bounce signal can be seen in the raw data. However, the signal from ground bounce was removed from the corrected data.

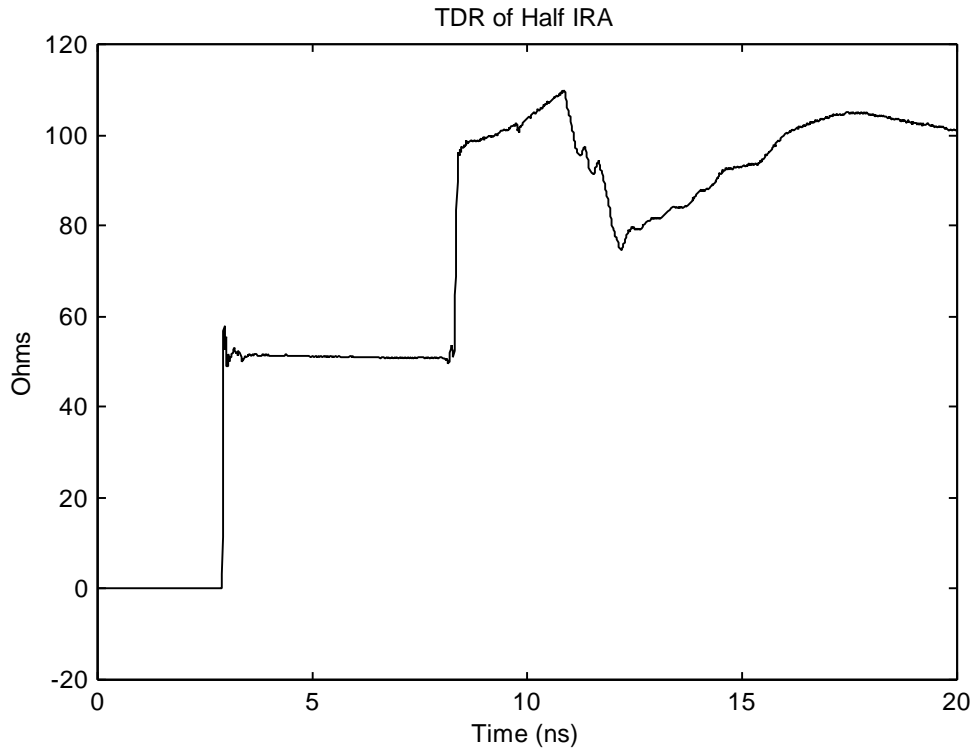


Figure 2.1 TDR of HIRA.

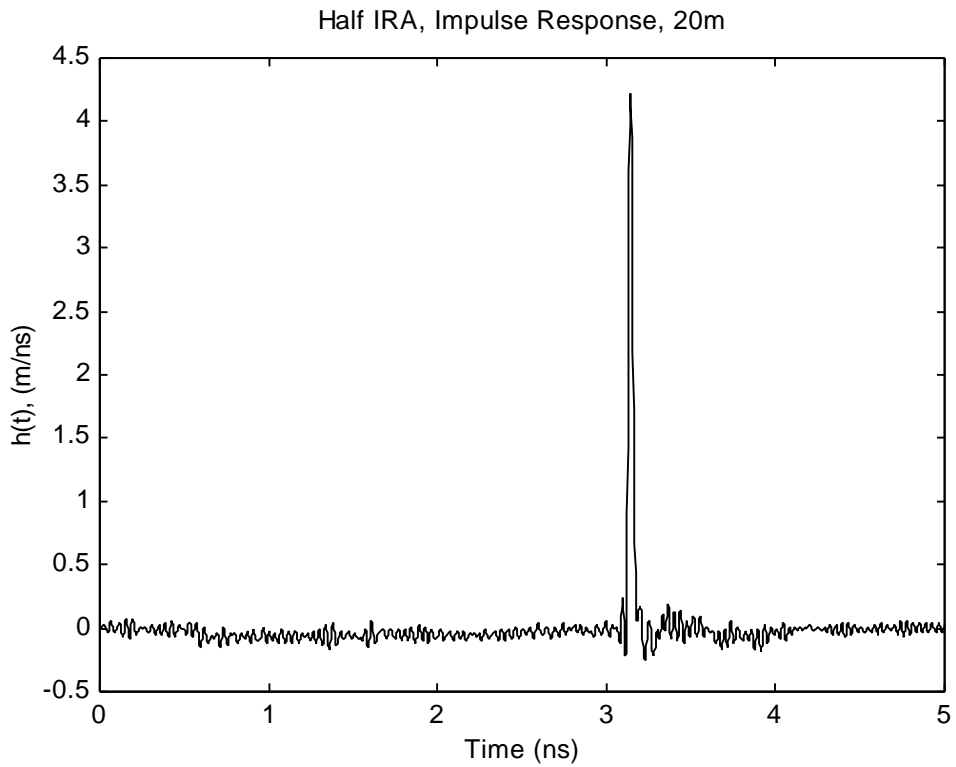


Figure 2.2 HIRA Impulse Response ($h_{HIRA}(t)$) on Boresight.

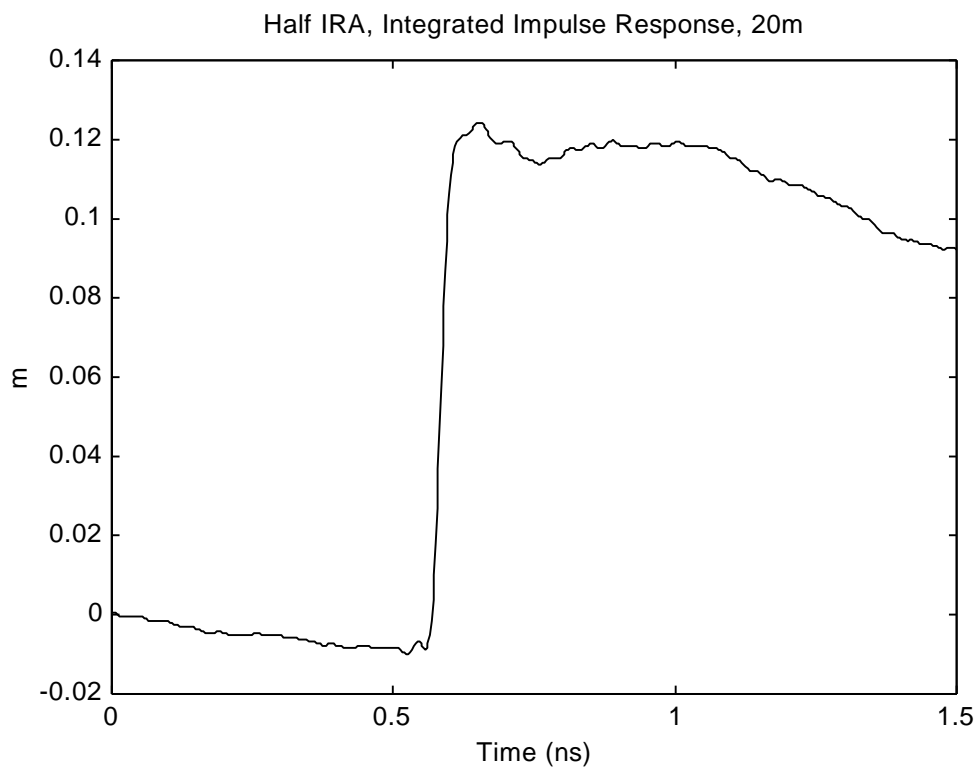


Figure 2.3 $h_{\text{HIRA}}(t) dt$, Effective height 0.13m.

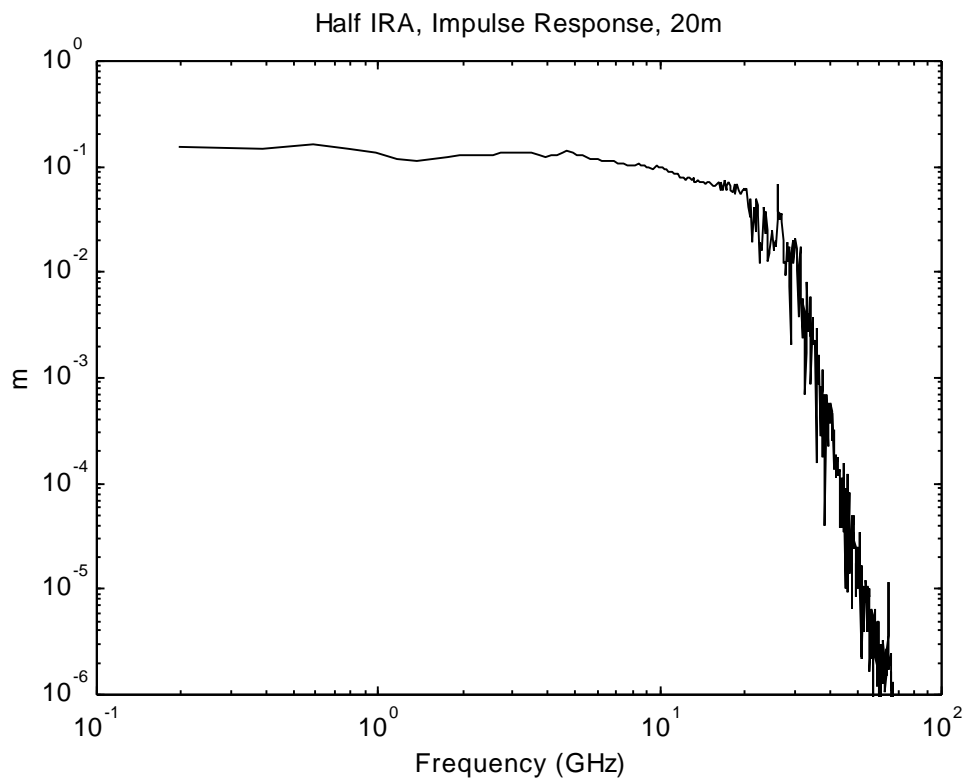


Figure 2.4 HIRA Impulse Response in Frequency Domain.

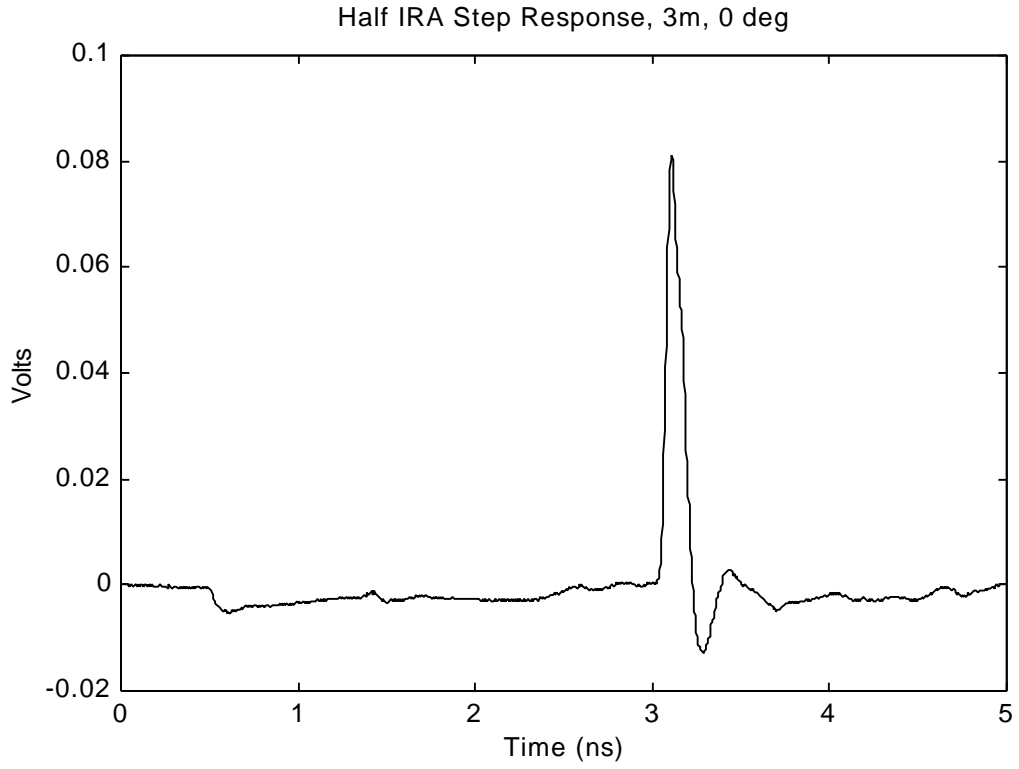


Figure 2.5. Measured Voltage on Boresight at 3 m.

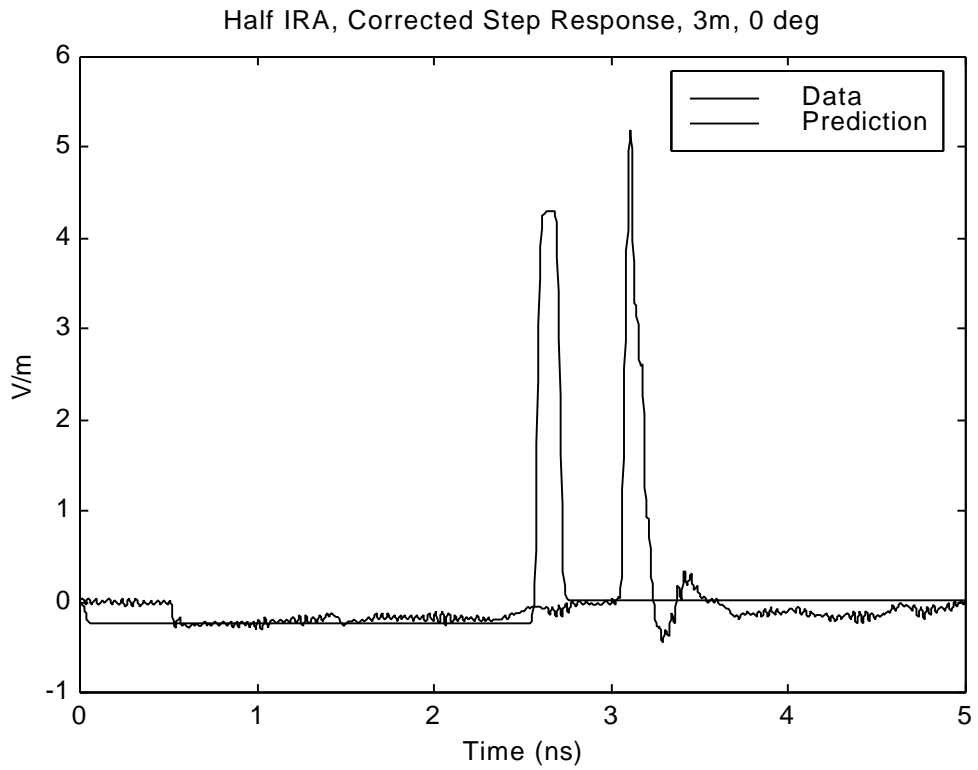


Figure 2.6. Comparison of Corrected Data and Prediction.

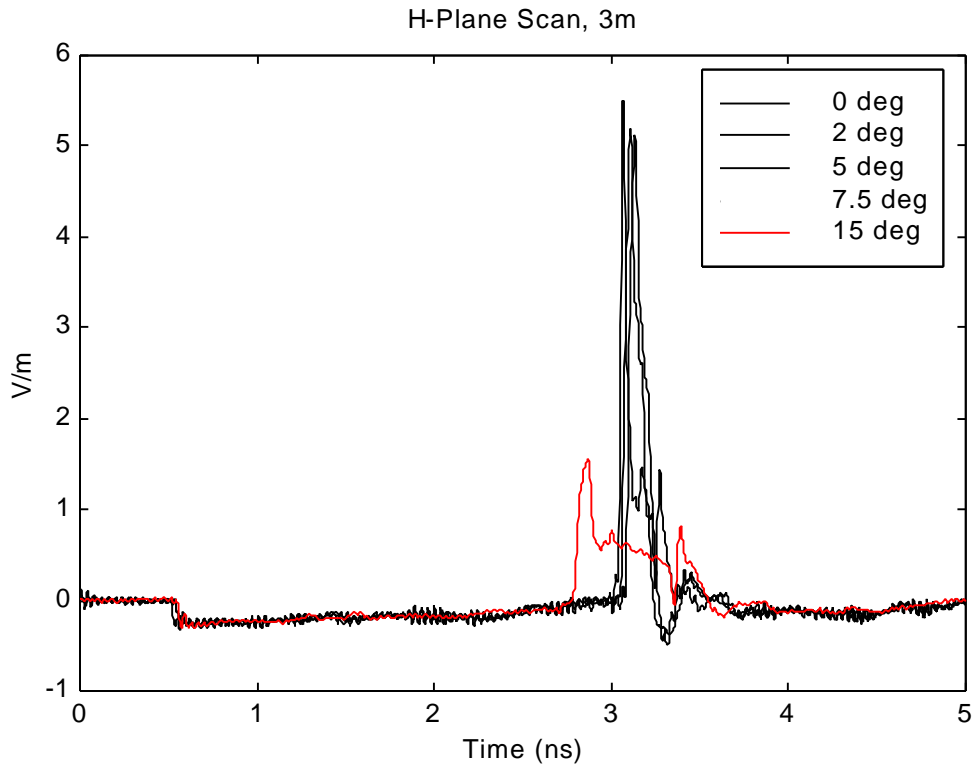


Figure 2.7. H Plane Scan at 3 m.

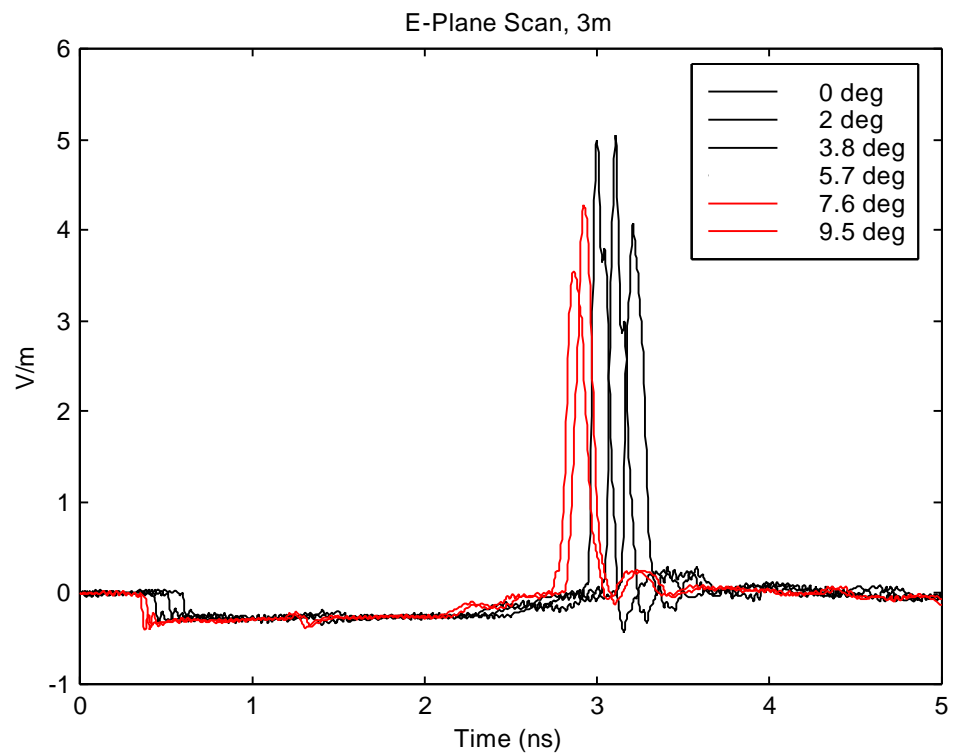


Figure 2.8. E Plane Scan at 3 m.

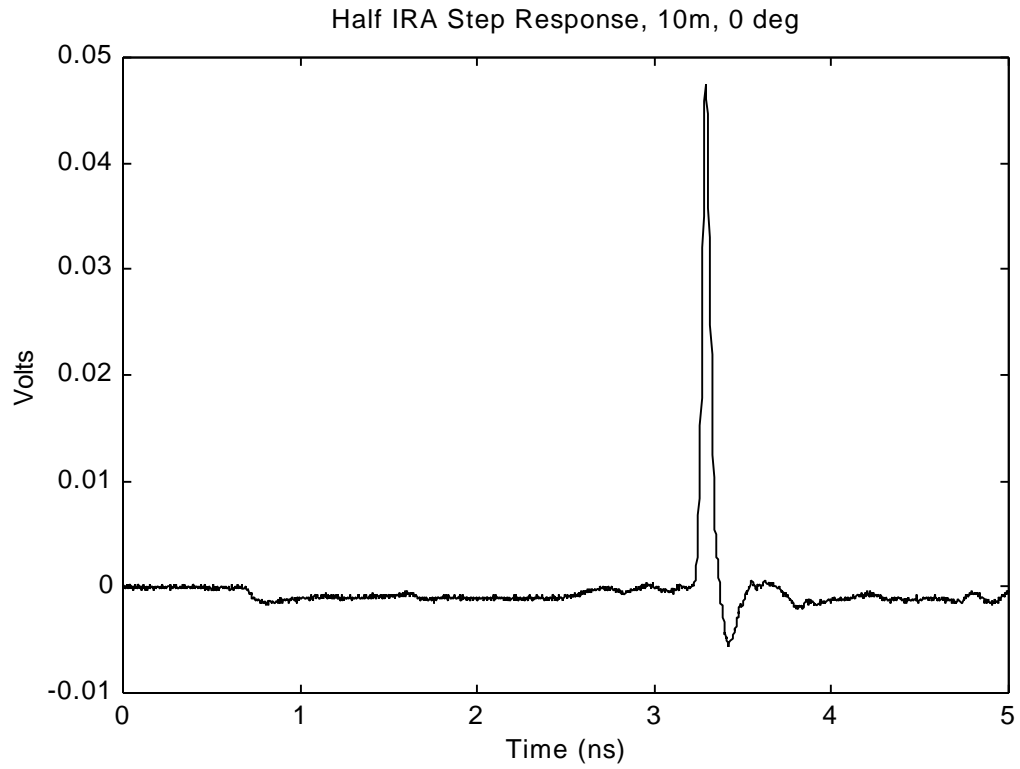


Figure 2.9. Measured Voltage on Boresight at 10 m.

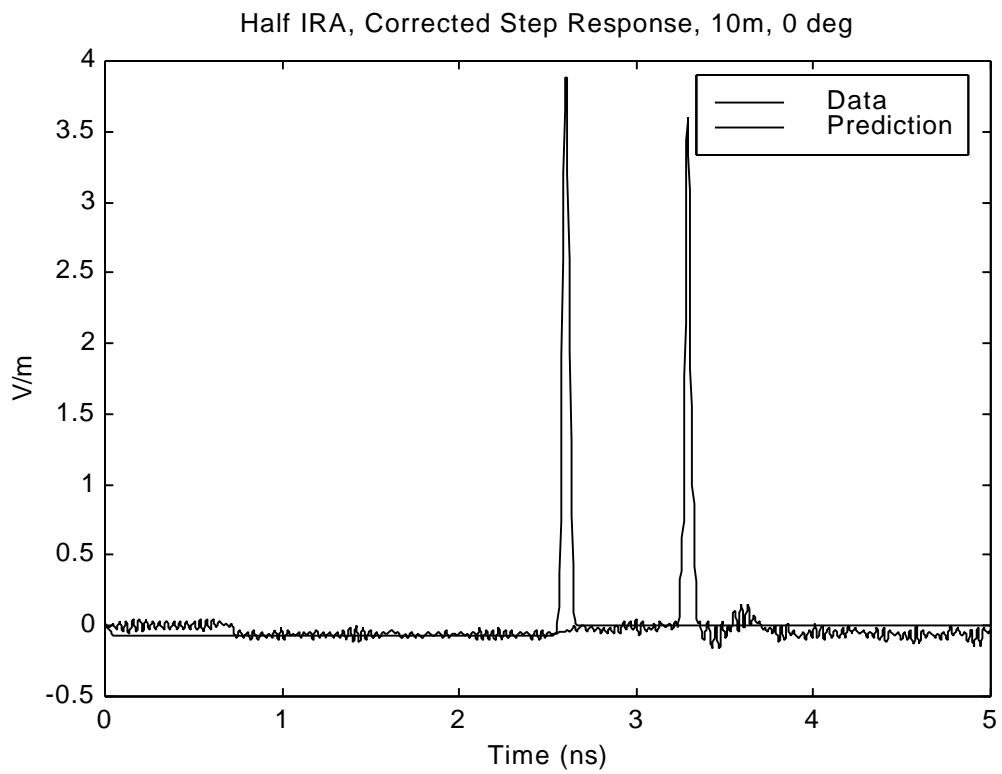


Figure 2.10. Comparison of Corrected Data and Prediction.

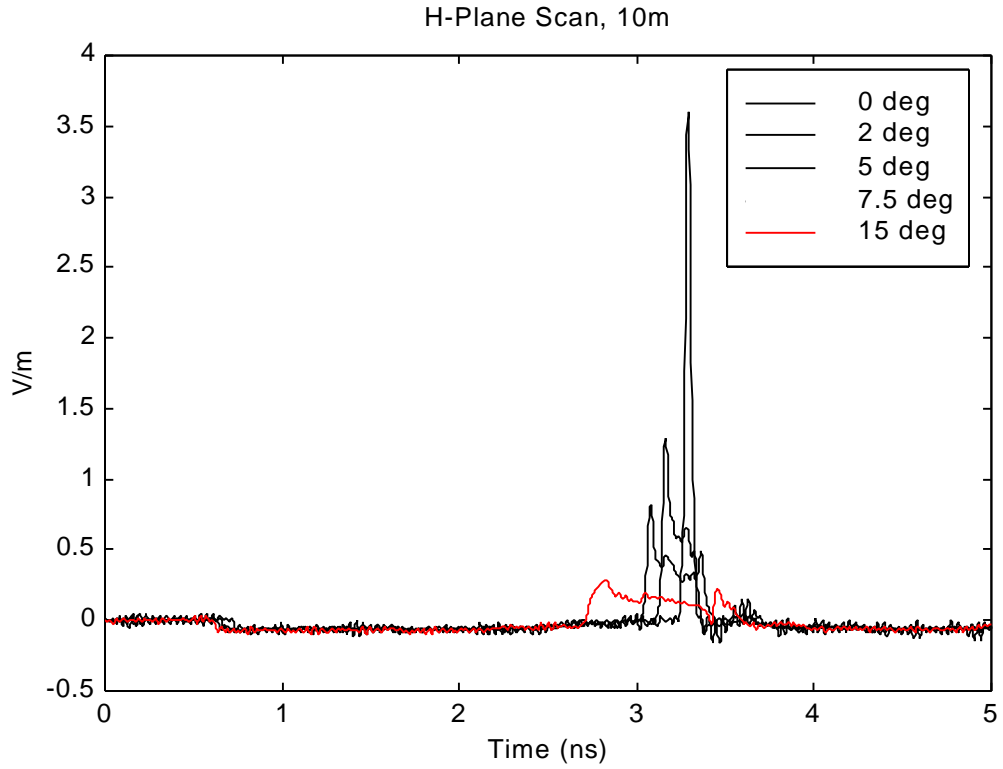


Figure 2.11. H Plane Scan (to right) at 10 m.

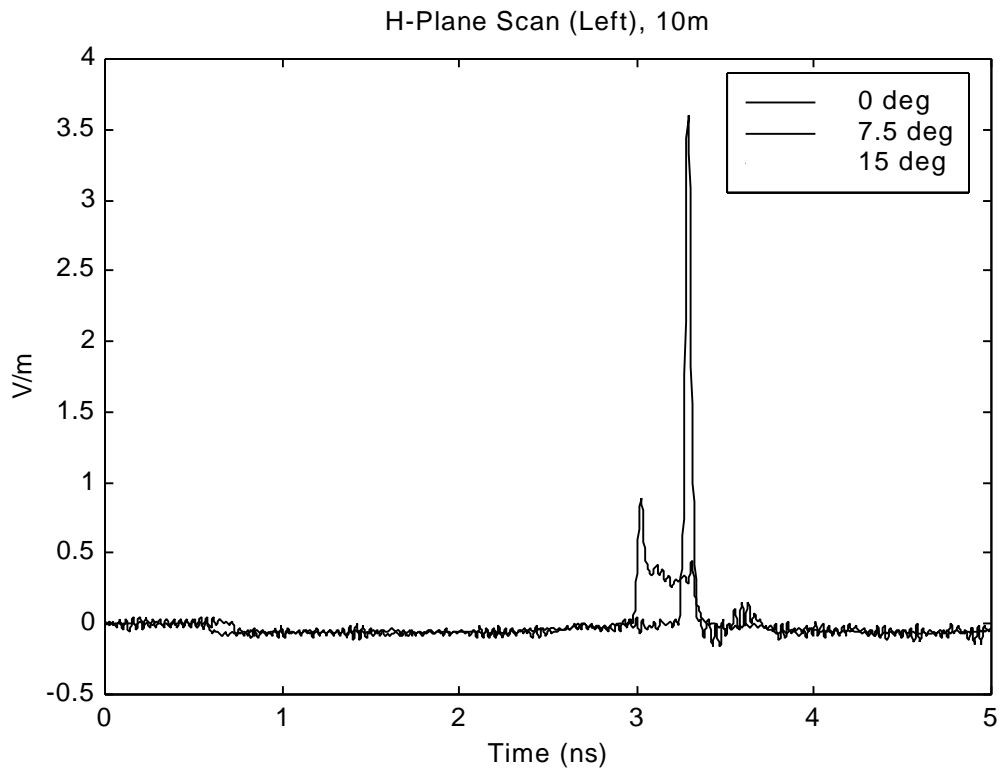


Figure 2.12. H Plane Scan (to left) at 10 m.

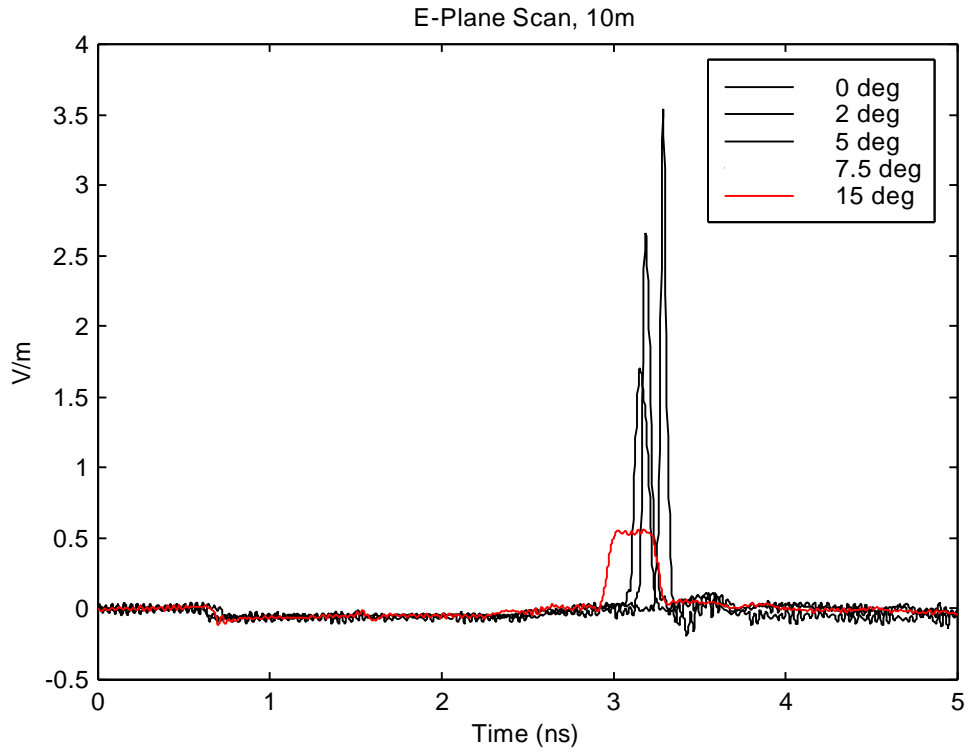


Figure 2.13. E Plane Scan (skyward) at 10 m.

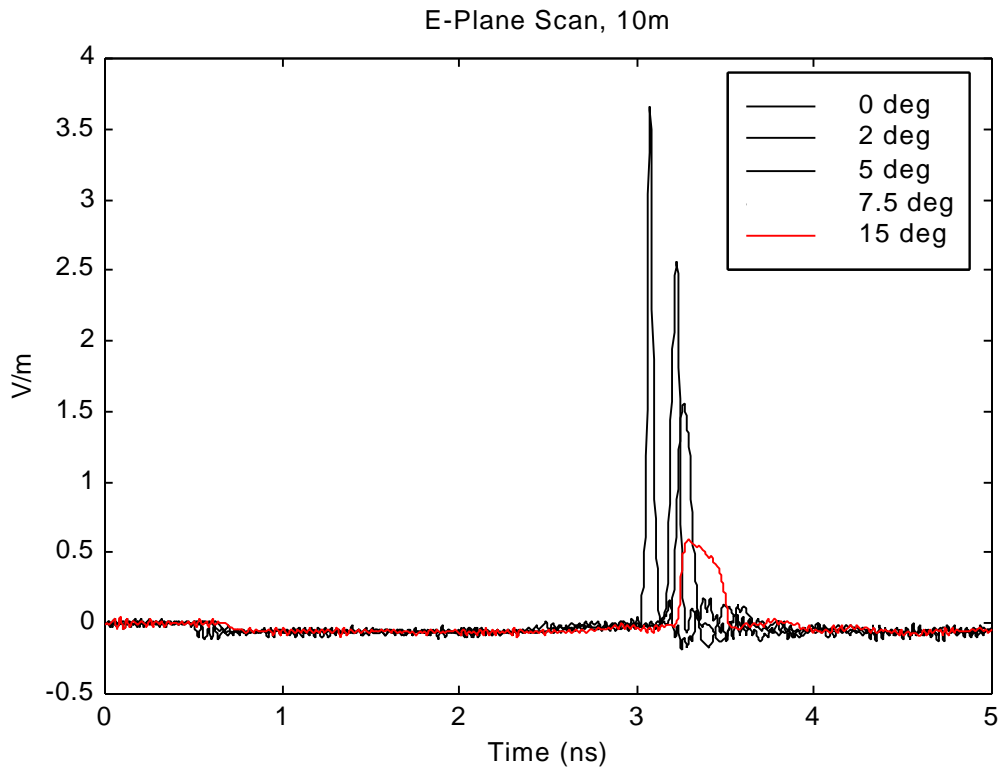


Figure 2.14. E Plane Scan (downward) at 10 m.

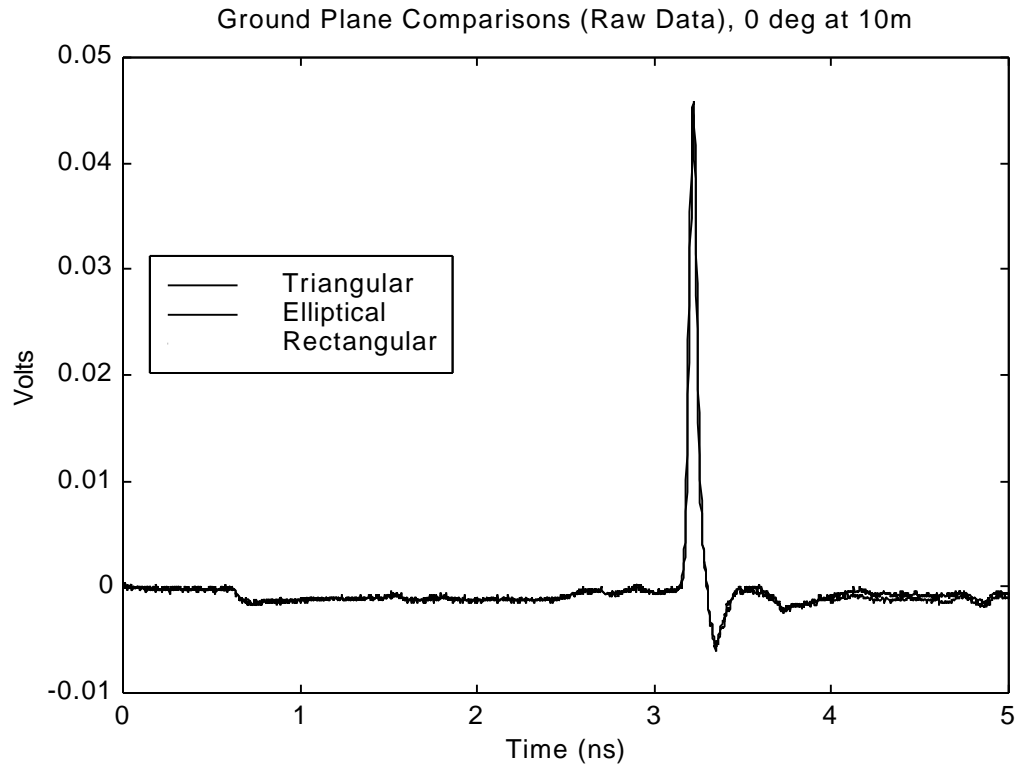


Figure 2.15. Comparison of Ground Plane Configurations.

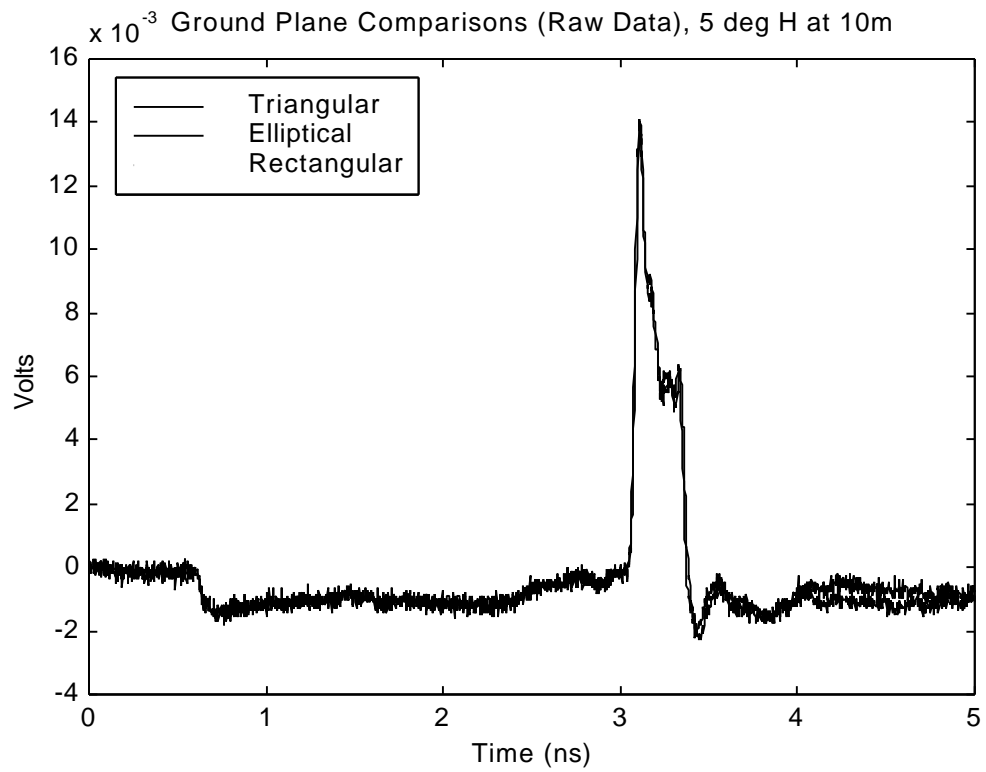


Figure 2.16. Comparison of Ground Plane Configurations.

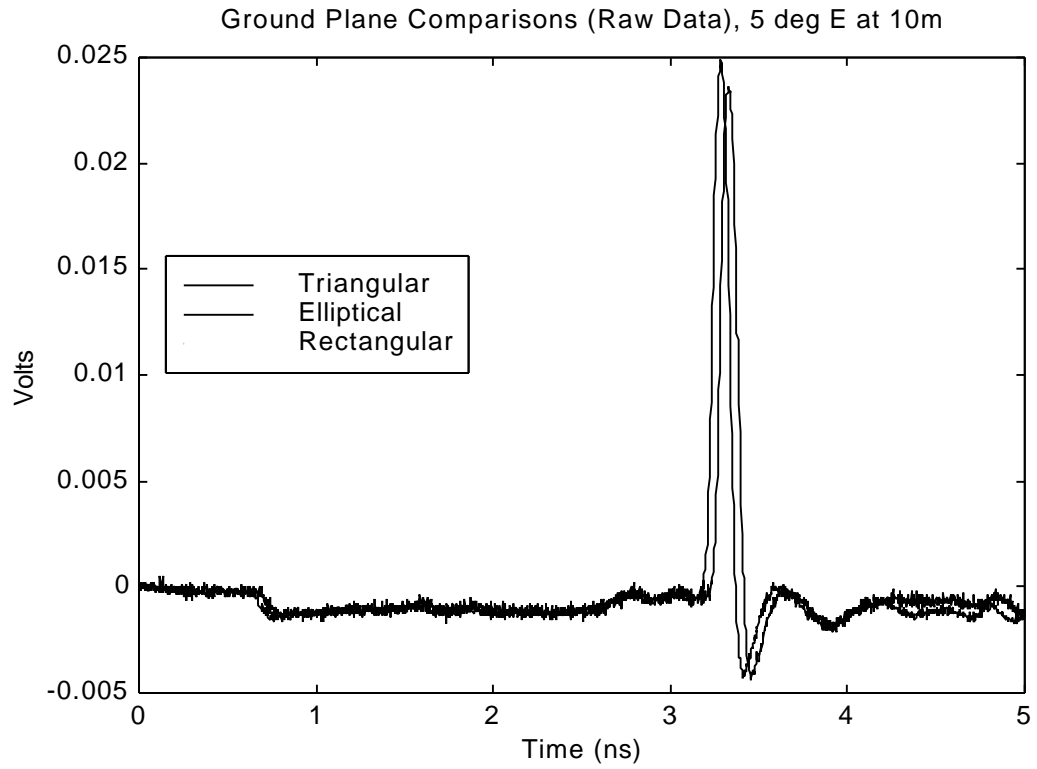


Figure 2.17. Comparison of Ground Plane Configurations.

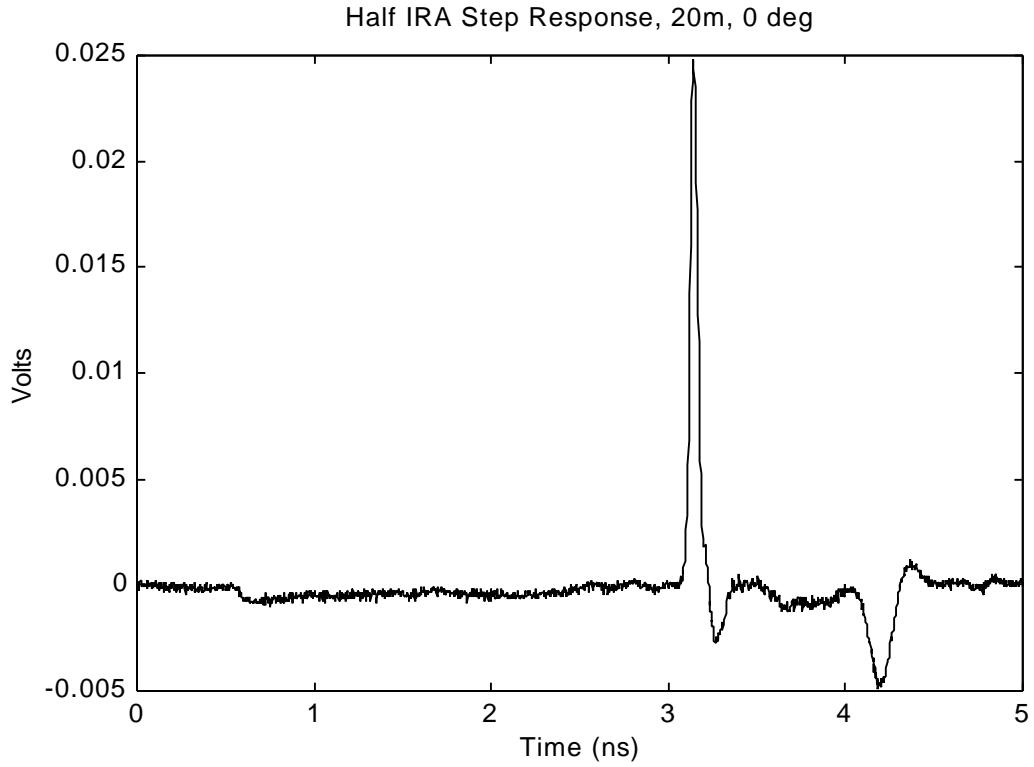


Figure 2.18. Measured Voltage on Boresight at 20 m Showing Ground Bounce.

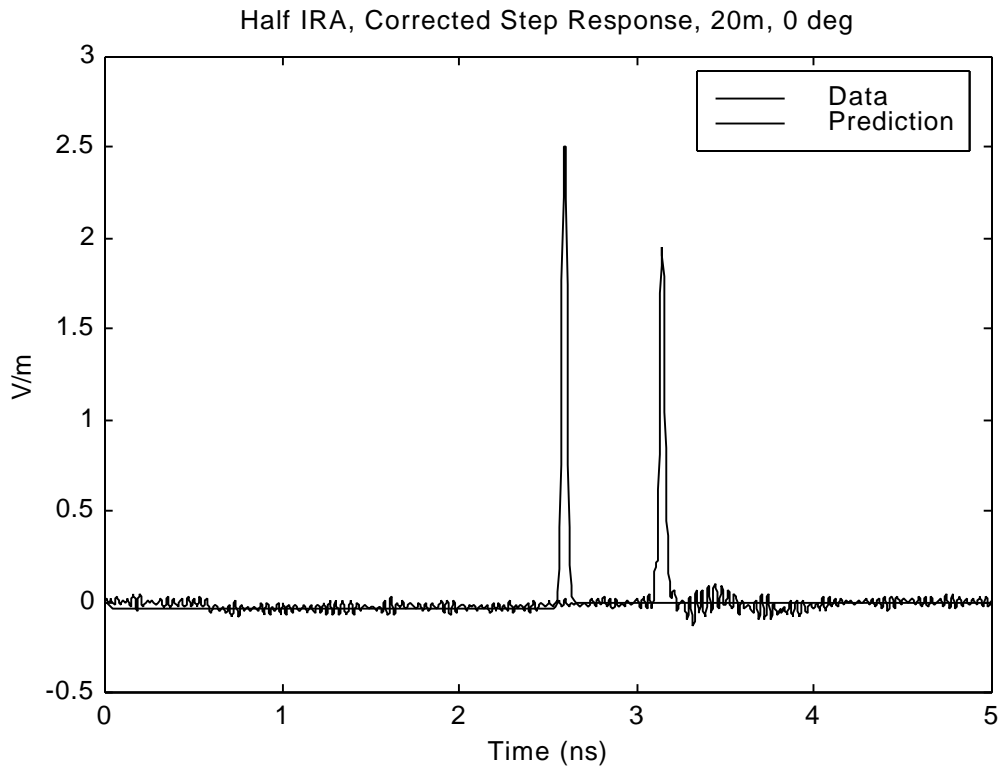


Figure 2.19. Comparison of Corrected Data and Prediction.

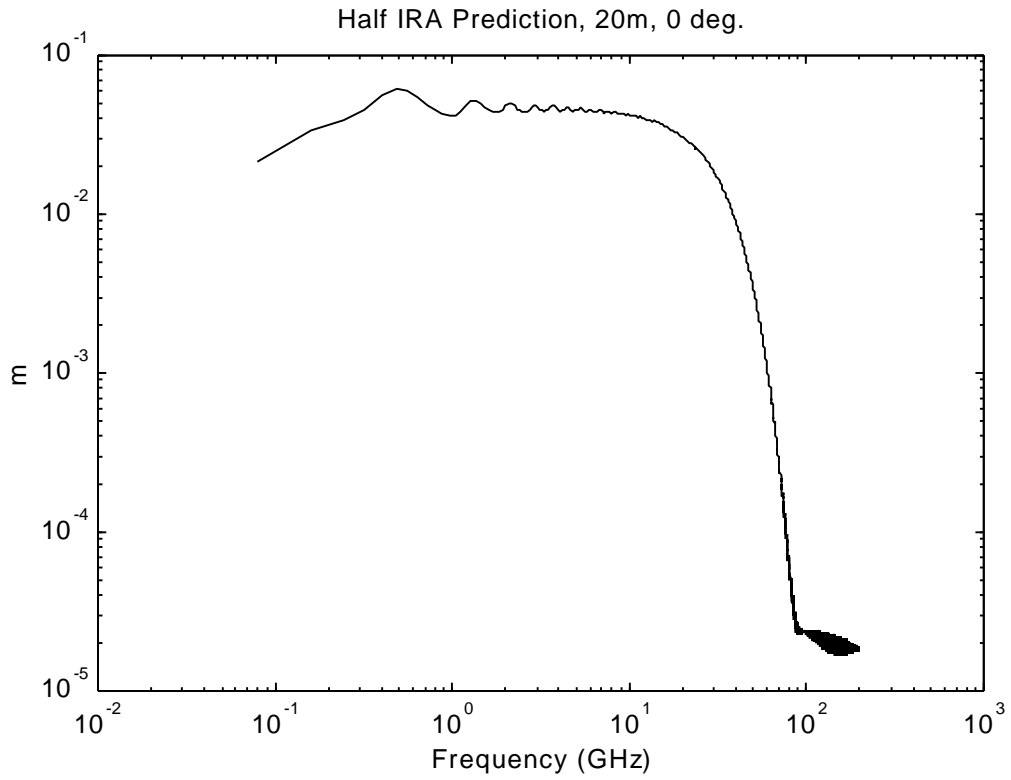


Figure 2.20. HIRA on Boresight Prediction at 20 m.

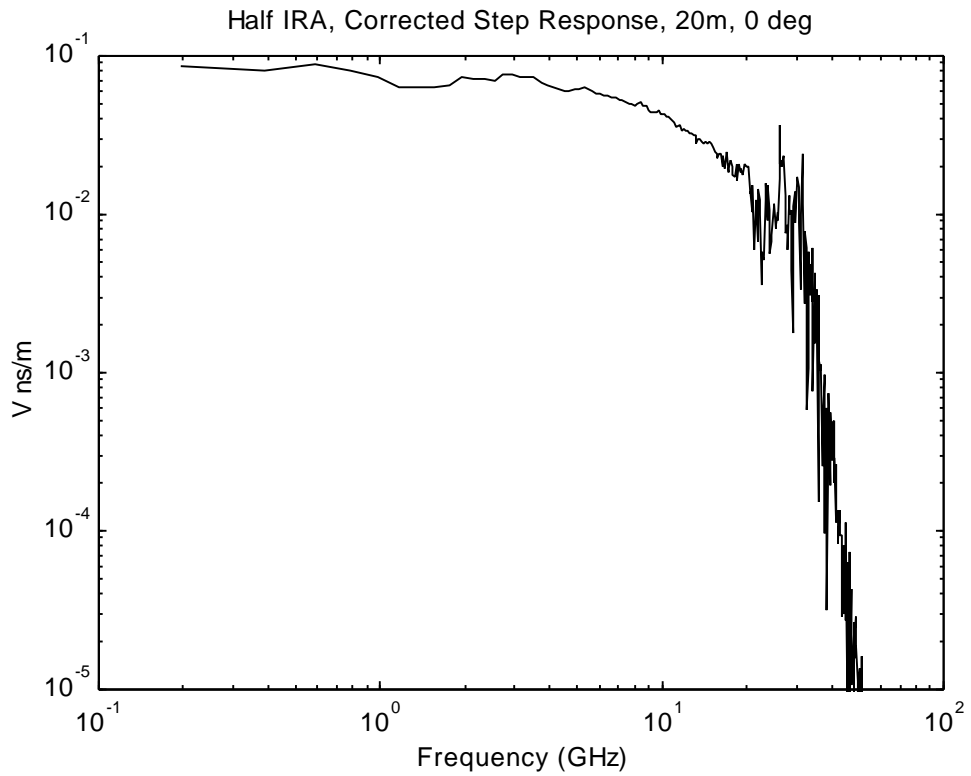


Figure 2.21. HIRA Corrected Step Response on Boresight at 20 m.

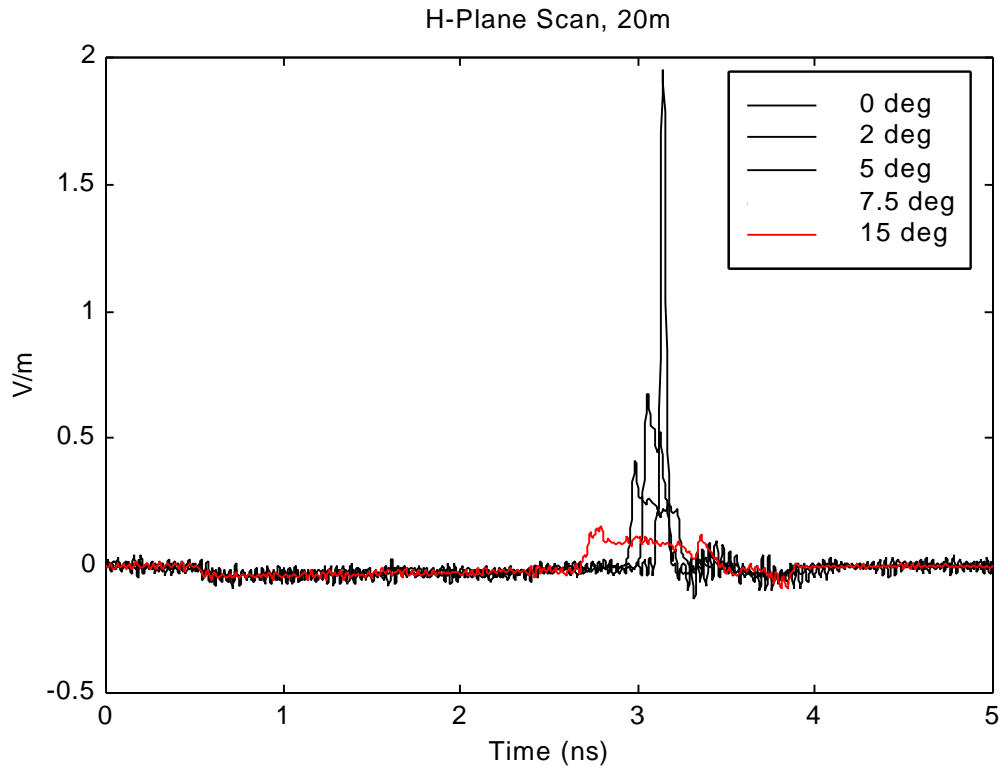


Figure 2.22. H Plane Scan at 20 m.

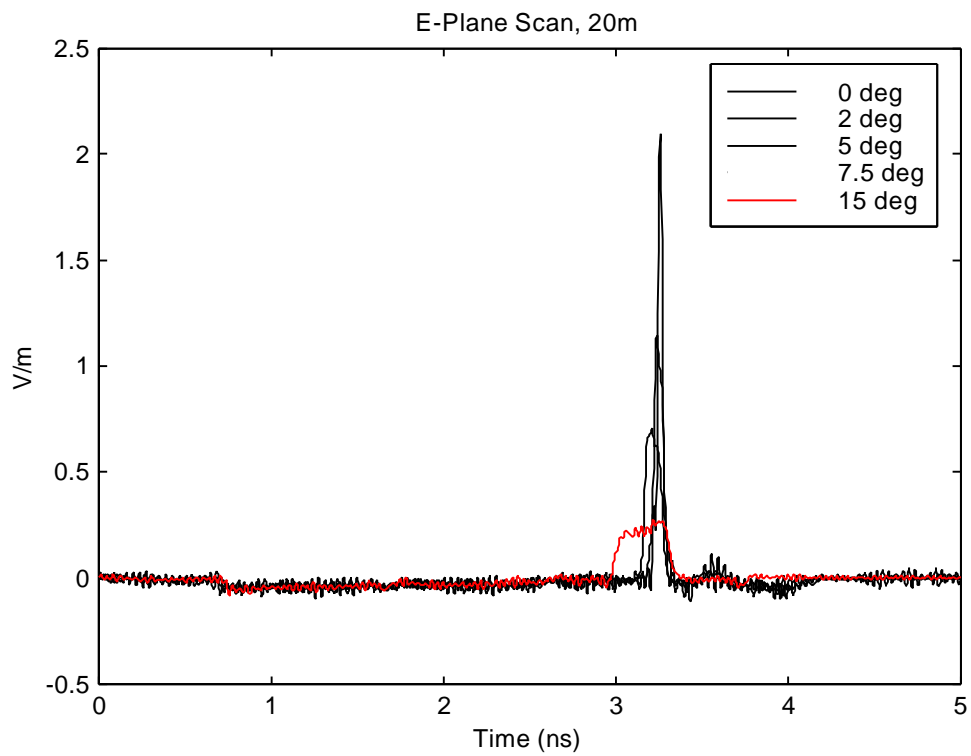


Figure 2.23. E Plane Scan at 20 m.

III. Conclusions

Table I gives the peak electric field and the FWHM for the corrected data and for the predictions made by Dr. Giri for the on boresight case at each distance. These values are based on the data vs. prediction comparisons shown in Figures 10, 14, and 23. The agreement between the measurements and the theory is very good, especially considering that Dr. Giri's calculations did not include all of the shadowing due to the feed elements.

Table I. Comparisons to Predictions

r (m)	Corrected Data		Predictions	
	Peak (V/m)	FWHM (ps)	Peak (V/m)	FWHM (ps)
3	5.2	96.6	4.28	128
10	3.6	35	3.88	44.8
20	1.95	31.5	2.5	34.5

The peak values of the corrected E fields at each angle (H and E plane scans) were used to estimate the angle at which 50% power (0.707 peak voltage) and 50% peak voltage occurred at the 10 m and 20 m ranges. This angle was used to compute a spot size for each case. This information is presented in Table II where the angle given is the angle off boresight (half angle) and the spot size is the diameter ($2*r*\tan(\text{angle})$).

Table II. Spot Size

r (m)	H Plane				E Plane			
	50% Power		50% Voltage		50% Power		50% Voltage	
	Angle (°)	Diameter (m)	Angle (°)	Diameter (m)	Angle (°)	Diameter (m)	Angle (°)	Diameter (m)
10	0.5	0.17	1.2	0.42	2.5	0.87	4.4	1.54
20	0.4	0.28	1.0	0.70	1.2	0.84	2.8	1.96

References

1. E. G. Farr, C. E. Baum, and W. D. Prather, Multifunction Impulse Radiating Antennas: Theory and Experiment, Sensor and Simulation Note 413, November 1997.
2. David V. Giri, private communication.
3. O. V. Mikheev, et. al., New Method for Calculating Pulse Radiation from an Antenna With a Reflector, IEEE Trans. Electromag. Compat., Vol. 39, Feb. 1997, pp. 48-54.
4. C. E. Baum, A Symmetry Result for an Antenna on a Truncated Ground Plane, Sensor and Simulation Note 415, November 1997.